X-ray photoelectron spectroscopy (XPS) studies of initial stages of copper deposition from bis(hexafluoro-acetylacetonato)copper(II) (Cu(hfac)$_2$) on Si(111)-7×7 at room temperature. Part C

C. IONESCU[*], M. A. IONESCU, I. CIUCA
Faculty of Science and Materials Engineering, Politehnica University of Bucharest, Romania

Organometallic chemical vapour depostion (OMCVD) of copper compounds is the preferred method for metallization of semiconductors over physical vapour deposition. The advantages of CVD are selectivity and ambient conditions for deposition (low vacuum and room temperature). UPS and XPS spectra of Cu deposited from Cu(hfac)$_2$ via chemical vapour deposition onto Si(111)-7x7 were studied for apparent exposures of 0.02, 0.04, 0.06, 0.08, 0.1 L at room temperature. Cu(hfac)$_2$ adsorption on Si(111)-7x7 at RT follows a ligand dissociative pathway with ligand fragmentation. At low exposures (i.e. 0.04 L) the precursor adsorbs onto Si surface in the reduced form, probably as Cu(I). This is supported by the absence of the shake-up features in the Cu XPS spectrum. Also Cu(II) was accounted for 5% of the total amount of Cu. The driving force for the reduction (Cu(II) → Cu(I)) is the Si(111) surface in its 7x7 reconstructed form. The process takes place at electron states on adatoms in Takayanagi's model. The reaction products at the end of deposition at the surface are: ligands (L), fragmented ligands (L$_f$), Cu(I)(hfac) (Cu-L), and copper (Cu). The fact that the Cu(II) intensity is constant over all depositions while the Cu(I) intensity continues to grow from one depostion to the other suggests that Cu(I) is associated with ligands or fragments of ligands. Cluster growth terminates via ligand saturation. This is our explanation to the "magic " number Cu cluster described by Horton et al. (6).

(Received August 25, 2011; November 23, 2011)

Keywords: Chemical vapour deposition, Copper, Low index single crystal Si surfaces, Ultraviolet photoelectron Spectroscopy, X-ray photoelectron spectroscopy, Takayanagi's model

1. Introduction

Organometallic chemical vapour deposition (OMCVD) of copper compounds (1,2,3,4,5) was explored for metallization of semiconductors in microelectronics via the deposition of (hexafluoroacetylacetonato)copper(II) (Cu(hfac)$_2$), hfac$^-$ = [CF$_3$OCHCOCF$_3^-$], a bidentate ligand and the related Cu(I) compound hexafluoroactetylactonato (1,5 octadiene) copper(I) ((hfac)Cu(COD)) (6, 7).

In our ultraviolet photoelectron spectroscopy (UPS)) study of the Cu(hfac)$_2$ interaction with Si (111)-7x7 Part A (8, 9,10, 35) we concluded that the peak at -17 eV is the secondary electron peak and its variation with the exposure reflects changes in the secondary electron emission caused by the presence of Cu (I) and fluorinated moities.

A previous study performed at various temperatures (6) (below the Cu dissolution temperature) has shown that the Cu(hfac)$_2$ deposits on the Si(111)-7×7 showing a physical separation between the Cu (which forms clusters of 8-10 atoms) and the ligands which also appear to be aggregated. The structure and hence the quality of the metallic film is controlled by nucleation and growth processes at the initial stages of growth. Our goal was to understand the mechanism of initial stages of the

Cu(hfac)$_2$ deposition at room temperature (RT). A number of questions are addressed in the present study:

-    In the case of a dissociative adsorption will the ligand adsorb intact or it will adsorb as smaller molecular fragments?

-    In the case of a dissociative adsorption will the growth of clusters terminate via saturation of Cu clusters with ligands or fragments of ligands? In other words which is the key to the formation of the so-called magic number clusters reported by Horton *et al*. (6)

2. Experimental details

The experiments were carried out in a home built ultra high vacuum (UHV) chamber which contains a differentially pumped He-discharge lamp, XPS capabilities and other standard surface science tools identical to those on which we performed our previous UPS and XPS experiments (34) (35). Si sample was processed using the same recipe we employed for the UPS and XPS experiments (34) (35). Prior to deposition the precursor was conditioned in the same manner as for the previous experiments (34) (35).

The Si sample faced the doser at a distance of ~5 cm (similar to the one used for the previous Cu(hfac)$_2$

deposition studied by UHV-STM) (11) and the dosing was performed at room temperature in 21 sec. (i.e. 0.02 L) increments, until the compound in the reservoir evaporated totally. The amount deposited each time was approximately the same since the increase in the pressure during deposition was the same for each of the 5 depositions. The deposition time for each subsequent exposure to Cu(hfac)$_2$ was 21 sec. each time, and the sample was not flashed in between depositions; thus the coverage after the second deposition corresponded to an exposure time of 42 sec. (i.e. 0.04 L), the third of 63 sec. (i.e. 0.06 L), the fourth of 84 sec. (i.e. 0.08 L), and the fifth of 105 sec. (i.e. 0.1 L) respectively.

3. Results and discussion

After flashing the sample, the XPS spectra (34, 35) showed no C1s peak which would appear at 284.15 eV suggesting a surface free of C as contaminant. XPS also confirmed the absence of SiO$_2$.

3.1 XPS experiments (Part C)

Wide scans were taken, followed by narrow scans looking for an increase in the area under the Cu 2p$_{3/2}$XPS binding energy signal with the deposition time. Then the same procedure was done for C 1s, F 1s and O 1s (35). The signal for C 1swas weak throughout the entire experiment (the C 1s XPS spectra are not presented here) due to its small cross-section but enough to give semi-quantitative information that was correlated to UPS data (34).

The signal for Cu 2p$_{3/2}$ after the first deposition time was also weak so we started our investigation from the second deposition time (i.e. the 42 sec. deposition time or 0.04 L) and those data are presented here.

The overall deposition time was 105 sec. which corresponds to an exposure of 0.1 L.

Our previous study concluded that most dissociation of Cu(hfac)$_2$ and ligand fragmentation occurs at the beginning of deposition. At the end of the deposition, fluorine is quantitatively retained; i.e. the ratio F:Cu is close to that in the intact ligand. These observations support the proposed dissociative pathway with ligand fragmentation proposed for the Cu(hfac)$_2$ deposition on Si(111)-7×7 at room temperature (35).

One conclusion is immediate: at the end of the deposition, fluorine is quantitatively deposited; i.e. the ratio F:Cu is close to that in the intact ligand. The above observation regarding F 1s is also consistent with previous work of Cheng *et al.* (7). At T < 233 K their O 1s XPS data indicate that the ligand remains intact; F 1s XPS data for the same temperature indicates only slight changes in the binding energy. Above 288 K, the temperature at which we performed our experiments, ligand fragmentation occurs, C-F bonds in CF$_3$ groups are being broken and the CF$_x$groups are generated, and hence F bonds to Si. Cohen *et al.* (13) reported ligand fragmentation via X-ray decomposition of the ligand.

Ligand fragmentation was also reported by Donnely *et al.* (14) and Parmeter (15).

The fact that F "sticks" more than oxygen on Si is thermodynamically consistent: the standard bond formation energy ΔH^0_f for the Si-F bond is -135 kcal/mol (or -564.84 kJ/mol) while that of Si-O is -108 kcal/mol (or - 451.87 kJ/mol) (16, 17, 18, 19).

3.2 Deconvoluted XPS Spectra for Copper

The XPS spectra for Cu 2p$_{3/2}$ (Figs. 1-4), O 1s (Figs. 5-8), and F 1s (Figs. 9-12) were deconvoluted using mixed Gaussian-Lorentzian functions with a linear background approach as provided by the XPS Peak Fitting Program Version 4.1.

The Cu 2p$_{3/2}$ XPS signal for the 0.02 L was weak so that we present here the 0.04, 0.06, 0.08 and 0.1 L data respectively. We follow the same procedure for O 1s, and F 1s XPS signal.

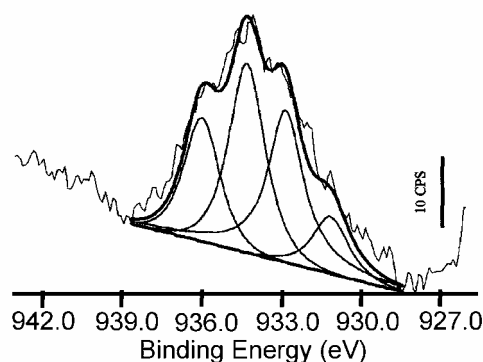The Cu 2p$_{3/2}$ XPS spectrum for the 0.04 L exposure (Fig. 1) shows after deconvolution four peaks:

Fig. 1. Cu 2p$_{3/2}$ XPS spectrum for a 0.04 L exposure of Cu(hfac)$_2$ on Si(111)-7x7at RT.
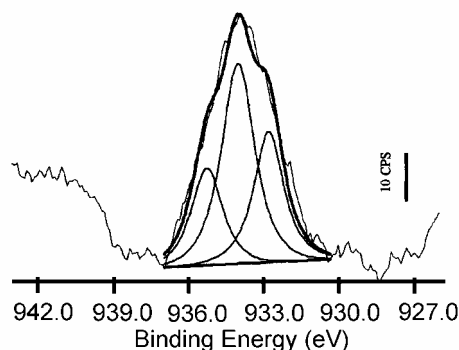
Fig. 2. Cu 2p$_{3/2}$ XPS spectrum for a 0.06 L exposure of Cu(hfac)$_2$ on Si(111)-7x7 at RT.

- 931.2 eV peak which disappears at exposure of 0.06 L or greater. The assignment of this peak is uncertain, but as it occurs at the lowest exposures, we tentatively assign it to very small Cu clusters or even individual Cu atoms bonded to Si;

- 932.8 eV which corresponds to Cu metal deposited on Si (20, 21, 22). Given the argument above, we assume that the copper is present as larger clusters characteristic of Cu metal on Si;

- 934.3 eV the main peak which corresponds to Cu(I) adsorbed on Si as Cu(I)(hfac) complex (6, 7, 23) and

- 936.0 eV which can be assigned to Cu(II) in Cu(hfac)$_2$ complex (6, 23).

The Cu 2p$_{3/2}$ XPS spectrum for the 0.06 L exposure (Fig. 9) shows after deconvolution three peaks:

- 932.8 eV - assigned as Cu metal (20, 21, 22); it shows a small increase in the intensity when comparing with the corresponding peak for the 0.04 L exposure, possibly by conversion of the copper responsible for the 931.15 eV peak to larger clusters;

- 934.0 eV - the main peak which corresponds to Cu(I) adsorbed on Si as Cu(I)(hfac) (6, 7, 33); it is more intense (almost doubles) than the corresponding peak in the 0.04 L spectrum; and

- 935.3 eV - the Cu(II) peak; it shows a very small increase compared to the corresponding peak in the 0.04 L spectrum (6, 23). The observation that the Cu(II) intensity stays almost constant while the Cu(I) intensity continues to increase from one deposition to another, is clear evidence that the Cu deposited in this exposure range is associated with ligands.
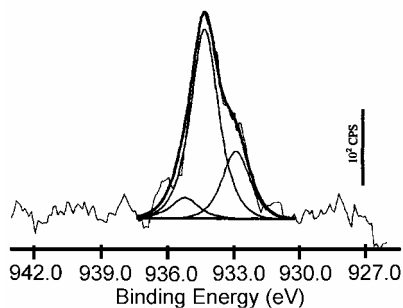

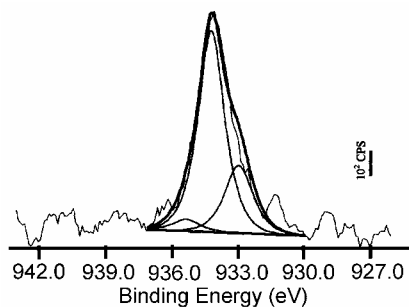*Fig. 3. Cu 2p$_{3/2}$ XPS spectrum for a 0.08 L exposure of Cu(hfac)$_2$ on Si(111)-7x7 at RT.*

Fig. 4. Cu 2p$_{3/2}$ XPS spectrum for a 0.1 L exposure of Cu(hfac)$_2$ on Si(111)- 7x7 at RT.

The Cu 2p$_{3/2}$ XPS spectrum for the 0.08 L exposure (Fig. 3) shows after deconvolution three peaks:

- 932.9 eV associated with the Cu metal (30, 31, 32) ; it shows an increase in the intensity compared to the corresponding peak for the 0.06 L exposure;

- 934.3 eV - the main peak which corresponds to Cu(I) adsorbed on Si as Cu(I)(hfac (6, 7, 33) and which is now almost six times more intense than the corresponding peak in the 0.06 L spectrum; and

- 935.3 eV - the Cu(II) peak (6, 23); it shows almost no increase compared to the corresponding peak for the 0.06 L exposure.

The Cu 2p$_{3/2}$ XPS spectrum for the 0.1 L exposure (Fig. 4) shows after deconvolution three peaks:

- 932.9 eV associated with the Cu metal (30, 31, 32); it shows an increase in the intensity compared to the corresponding peak for the 0.08 L exposure;

- 934.2 eV - the main peak which corresponds to Cu(I) adsorbed on Si as Cu(I)(hfac) (6, 7, 33) and which is triple the corresponding peak in the 0.08 L spectrum; and

- 935. 3 eV – the Cu(II) peak (6, 23); it shows almost no increase compared to the corresponding peak for the 0.08 L exposure (Table 1).

Table 1. Height of Cu(I) and Cu(II) peaks in counts/second as retrieved from the corresponding

Cu 2p$_{3/2}$ XPS spectra are: a) for 0.04L - Cu(I) 25.9 cps and Cu(II) 18.0 cps; b) for 0.06L - Cu(I) 42.0 cps and Cu(II) 20.4 cps; c) for 0.08L - Cu(I) 249.0 cps and Cu(II) 30.0 cps; d) for 0.1L – Cu(I) 783.0 cps and Cu(II) 42.0 cps.

The question arises as to why the Si surface reduces Cu(II) to Cu(I). Semiconductors have an energy gap around the Fermi level. In the case of the 7x7 reconstructed surface, electronic states

The question arises as to why the Si surface reduces Cu(II) to Cu(I). Semiconductors have an energy gap around the Fermi level. In the case of the 7x7 reconstructed surface, electronic states of Si are within this gap and this is why the Si(111)-7×7 surface exhibits a metallic character (21, 24). The metallic character is manifested in terms of a continuum of electron states near the Fermi level - energy levels that are close to each other. We believe that it is this metallic character that is the driving force for the reduction Cu(II) → Cu(I). The origin of "precursor splitting" into Cu and the (hfac) ligand, followed by (hfac) bonding to Si as smaller molecular fragments or to Cu clusters and Cu deposition onto the Si surface, might reside in the electron states on adatoms in Takayanagi's model. In our work, we described Cu clusters of specific size sitting in the faulted halves of the Si (111)-7x7 unit cell (Semenov et al.(11) similar to the size of clusters reported by Horton et al. (6)

The intensity of the Cu(II) signal remains constant while the intensity of the Cu(I) signal increases dramatically from one deposition to another (Table 2a, b, c, and d).

This supports the hypothesis that the cluster growth terminates via cluster saturation with ligands, and could therefore be the origin to the observation of a maximum cluster size reported by Horton *et al.*(6) in 1996. At low coverage a mechanistic approach to this problem is presented at the end of this article.

Table 2a, b, c, and d. Peak areas under each of the deconvoluted peaks for Cu for each of the corresponding deposition times are:

a) for 42 sec under the peak at 931.15eV - 16.33; under the peak at 932.84 eV -56.44; under the peak at 934.30 eV – 55.42; under the peak at 936.03 eV - 34.51. Total area = 112.7 b) for 63 sec under the peak at 932.81 eV - 48.24; under the peak at 934.03 eV - 79.87; under the peak at 935.27 eV - 35.66. Total area = 163.77 c) for 84 sec under the peak at 932.88 eV -164.03; under the peak at 934.30 eV - 489.12; under the peak at 935.20 eV - 52.24. Total area = 705.39. d) for 105 sec under the peak at 932.94 eV - 295.11; under the peak at 934.19 eV - 831.39; under the peak at 935.32 eV -52.24. Total area = 1179.04.

3.3 Deconvoluted XPS Spectra for Oxygen

Figs. 5-8 show the O 1sXPS spectra of oxygen deposited on Si(111)-7x7 from $Cu(hfac)_2$ at room temperature. The O 1s XPS spectrum for 0.04 L (Fig. 5) shows three peaks:
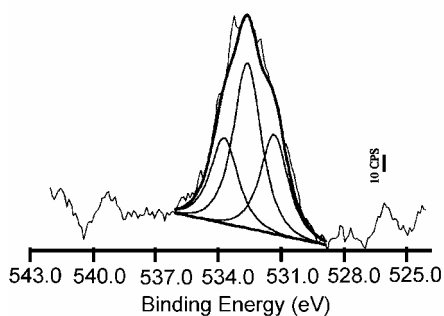

Fig. 5. O 1s XPS spectrum for a 0.04 L exposure of Cu(hfac)$_2$ on Si(111)- 7x7 at RT.
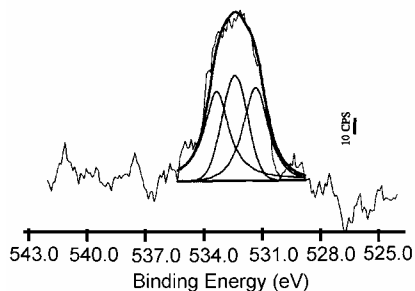

Fig. 6. O 1s XPS spectrum for a 0.06 L exposure of Cu(hfac)$_2$ on Si(111)-7x7 at RT.

- 531.3 eV that cannot be associated to $Cu(OH)_2$ or to Cu_2O since we did not detect any $Cu(OH)_2$ or Cu_2O in the Cu $2p_{3/2}$ XPS spectra; therefore this peak can be assigned to O in the Cu(II) intact precursor (not bonded to Si surface).
- 532.6 eV that can be associated with O in the intact hfac ligand; and
- 533.7 eV that can be associated with O in a non-oxygen surface bound $COCF_3$ fragment, or impurity oxygen. The presence of water (water of hydration via incomplete dehydration or rehydration) is accounted as source of oxygen.

The O 1s XPS spectrum for the 0.06 L (Fig. 6) reveal after deconvolution similar peaks to those shown in Fig. 1 for the 0.04 L exposure:
- 531.3 eV that can be associated to O in the $Cu(II)(hfac)_2$.
- 532.4 eV that can be associated with O in the intact hfac ligand; and
- 533.34 eV that can be associated with O in a non-oxygen surface bound $COCF_3$ fragment, or impurity oxygen.

The O 1s XPS spectrum for the 0.08 L (Fig. 7), and for the 0.1 L exposure (Fig. 8) reveal, after deconvolution, two peaks (possibly with a very weak third component) each:
- higher binding energy around 533.5 eV and around 533.4 eV in the 0.08 L spectrum and 0.1 L spectrum respectively; and
- lower binding energy around 532.2 eV and 532.3 eV in the 0.08 L spectrum and 0.1 L spectrum respectively.
All the above O 1s XPS assignments are consistent with those reported in literature (6, 7, 26, 27).

In the above O spectra the dominant O species is the O in Cu(I)(hfac) complex (Table 3a, b, c, and d) supporting the fact that the cluster growth terminates via cluster saturation with ligands.
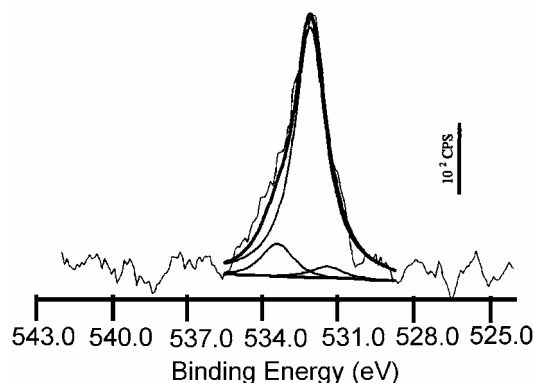

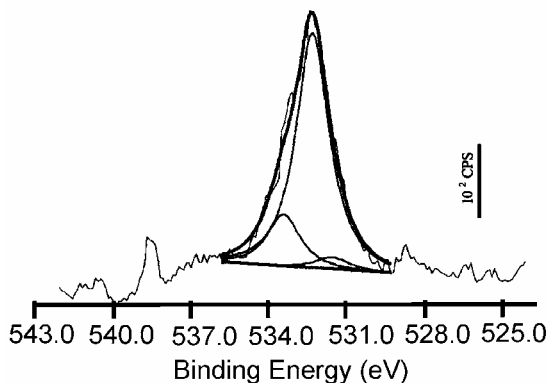*Fig. 7. O 1s XPS spectrum for a 0.08 L exposure of Cu(hfac)$_2$ on Si(111)-7x7 at RT.*

Fig. 8. O 1s XPS spectrum for a 0.1 L exposure of Cu(hfac)₂ on Si(111)-7x7 at RT.

Table 3 a, b, c, and d. Peak areas under each of the deconvoluted peaks for O for each of the corresponding deposition times are:

a) for 42 sec under the peak at 531.32 eV - 89.99; under the peak at 532.61 eV - 149.42; under the peak at 533.71 eV - 78.62. Total area = 318.03. b) for 63 sec under the peak at 531.33eV - 95.22; under the peak at 532.40 eV - 97.97; under the peak at 533.34eV - 116.30. Total area = 309.49. c) for 84 sec under the peak at 531.48eV - 35.66; under the peak at 532.17 eV - 929.14; under the peak at 533.46 eV - 97.16. Total area = 1056.96 d) for 105 sec under the peak at 531.50eV- 37.09; under the peak at 532.25 eV - 856.50; under the peak at 533.38 eV - 173.69. Total area = 1067.28

Fluorine

Deconvoluted XPS Spectra for Fluorine

Fig. 9-12 show the F 1s XPS spectra of fluorine deposited on Si(111)-7x7 from Cu(hfac)₂ at room temperature.

The F 1s XPS spectrum for 0.04 L exposure (Fig. 9) shows five peaks:
-   685.85 eV that can be associated with F bonded on Si as mono-fluorosilicon (20, 21, 28, 29)
-   687.25 eV that can be associated with surface bound $COCF_3$ (27, 28, 30)
-   688.4 eV that can be associated with F in the intact ligand (27);
-   689.6 eV that can be associated with $[CF_2]_n$ where n ≤ 2 (some particles are CF_2 and others are $(CF_2)_2$) (20) ; and
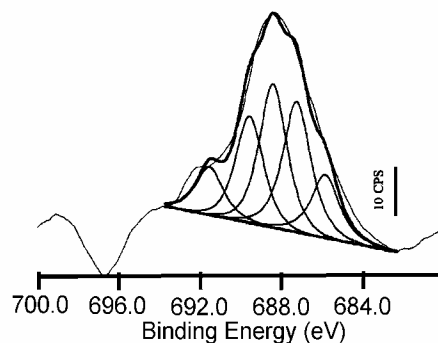-   691.56 eV that can be associated with $[CF]_n$ (20).

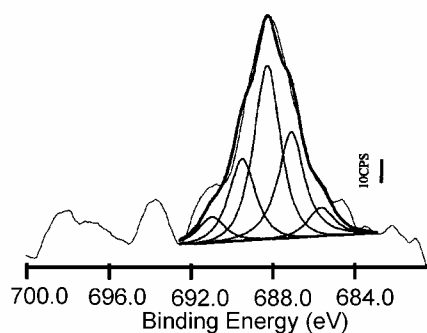*Fig. 9. F 1s XPS spectrum for a 0.04 L exposure of Cu(hfac)₂ on Si(111)-7x7 at RT.*

Fig. 10. F 1s XPS spectrum for a 0.06 L exposure of Cu(hfac)₂ on Si(111)-7x7 at RT.

The F 1s XPS spectrum for the 0.06 L (Fig. 10) exposure also shows five peaks:
-   685.65 eV that can be associated with F bonded on Si as mono-fluorsilicon (20, 21, 28, 29);
-   687.11 eV that can be associated with $COCF_3$ (26, 27, 30) ;
-   688.3eV that can be associated with F in the intact ligand (27);
-   689.6 eV that can be associated with $[CF_2]_n$ where n ≤ 2 (some particles are CF_2 and others are $(CF_2)_2$) (20) ; and
-   691.56 eV that can be associated with $[CF]_n$ (20).
The F 1s XPS spectrum for the 0.08 L (Fig. 11) and for the 0.1 L exposures (Fig. 12) reveals, after deconvolution, four peaks each:
-   around 685.8 eV that cannot be assigned to CuF_2 (20, 31), since CuF_2 was not detected in the Cu2p3/2 spectrum, nor to the CF_3 fragment. First, we did not assign the shift toward a lower binding energy to CF_3 groups since the value for its binding energy reported in literature (i.e. 689.6 eV or 689.67 eV (20, 32)) is far from our value. Therefore this peak is assigned to F bonded on Si.
-   687.2 eV respectively that can be assigned to $COCF_3$ bonded to Si (26, 27, 30);
-   688.4 eV that can be assigned to F in the intact ligand (27); and
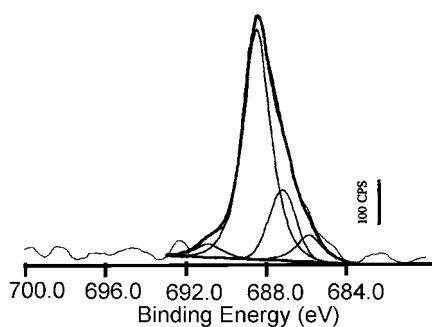-   690.9 eV and 690.8 eV respectively, that can be associated with $[CF]_n$ (20).

Fig. 11. F 1s XPS spectrum for a 0.08 L exposure of Cu(hfac)₂ on Si(111)-7x7 at RT.
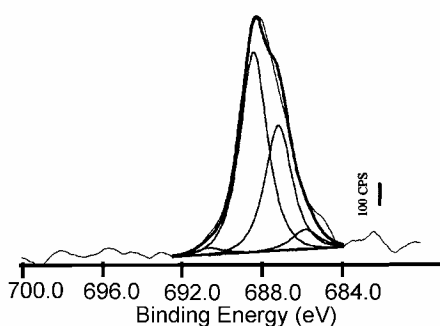
Fig. 12. F 1s XPS spectrum for a 0.1 L exposure of Cu(hfac)₂ on Si(111)-7x7 at RT.

The intensity of the F 1s XPS signal in the Cu(I)(hfac) species increases dramatically from one deposition to another (Table 4a, b, c, and d) suggesting again that the cluster growth terminates via cluster saturation with ligands. The presence of F on the Si surface is evidence that the precursor dissociation occurs probably during adsorption of the Cu(II)(hfac)₂ complex as Cu(I)(hfac). A similar observation was reported by Donnelly *et al. (14).*

Table 4a, b, c, and d. Comparative of peak area under each of the deconvoluted peaks for F for each of the corresponding deposition times are:

a) for 42 sec. under the peak at 685.85 eV - 25.03; under the peak at 687.25 eV - 50.76; under the peak at 688.42 eV - 53.84; under the peak at 689.58 eV - 39.52; under the peak at 691.56 eV -18.31. Total area =187.51.b) for 63 sec. under the peak at 685.85 eV - 20.48; under the peak at 687.11 eV - 80.17; under the peak at 688.29 eV - 123.40; under the peak at 689.50 eV - 58.11; under the peak at 690.98 eV - 18.13. Total area = 300.29. c) for 84 sec. under the peak at 685.84 eV - 113.79; under the peak at 687.18 eV - 282.44; under the peak at 688.45 eV - 1031.17; under the peak at 690.87eV - 59.35.
Total area = 1486.75. d) for 105 sec under the peak at 685.84 eV - 163.52; under the peak at 687.17eV - 1025.57; under the peak at 688.41 eV - 1651.95; under the peak at 690.61 eV - 54.20.
Total area = 2895.24.

F*rom* the above data (Figs. 9-12) an image of the chemistry at the Si surface can be derived:
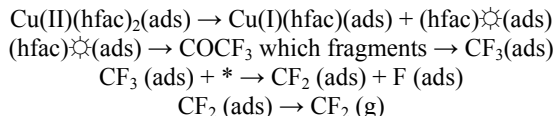
a)   at an exposure of 0.04 L   (Fig. 9) the surface shows fragmentation and dissociation of ligand. Most dissociation of Cu(hfac)₂ (semi-quantitatively: the Cu(hfac)₂ precursor loses one ligand which goes in the gas phase and the Cu(I)(hfac) species is created) and fragmentation of the (hfac) ligand occurs at this exposure.[CF]ₙ and F bonded to Si are the two species that are decreasing in intensity as the exposure is increased to 0.06 L. The broadening of the spectrum is explained by many electron states.

b)   at an exposure of 0.06 L (Fig. 10) the narrowing of the experimental peak (composed of five electron states) is evident. Lowering the concentration of the components (some electronic states are disappearing) namely the peak that appears at high binding energy ([CF]ₙ), the peak corresponding to [CF₂]ₙ (where n ≤ 2 (some particles are CF₂ and others are (CF₂)₂)) and that present at low binding energy (F) support the idea that fragmentation decreases as the exposure increases due to a decrease in the number of active sites.

c)   at the end of the deposition (i.e. the F 1s XPS spectra for 0.1 L exposure) some broadening of the experimental peak is observed when compared to the F 1s XPS spectra for 0.08 L exposure. The ratio for the peak responsible for broadening i.e. the peak assigned to the COCF₃ fragment in the F 1s XPS spectrum for 0.1 L (Fig. 12) and the height of the same peak for the 0.08 L exposure (Fig. 11) is 440cps/168cps = 2.6. We relate the growth of it to the growth in Cu(I)(hfac) and not to the Cu(II)(hfac)₂ (cross-section of Cu(I) and Cu(II) are almost the same) since the growth of Cu(II) increases only by a factor 1.4 (42cps/30cps) for the same exposures, and Cu(II) represents the only 5% (from the (783cps+42cps)) (Table 5) of the total Cu amount at the end of deposition. Possibly Cu(hfac)·(hfac) is being created (with the stoichiometry as that in Cu(hfac)₂) as a result of the decreased reactivity via saturation of active sites on clean Si and Cu clusters. This might be an explanation to the F:Cu ratio observed at the end of the deposition (i.e. 0.1 L exposure). This is close to that in the intact precursor (35). No fragmentation is present at this exposure since the surface reactivity should be considerably decreased due to a decrease in the number of active sites. The fragments that appear on the surface are species previously created at lower coverages.

In order to determine if the ligands adsorb intact or are fragmented, additional IR experiments should be performed. Taking into account the surface dipole selection rule, the (hfac) ligands which bond on the Si surface (if the ligand is not fragmented) would adopt an essentially upright geometry revealed in the reflection absorption infrared (RAIR) spectrum by one strong C-F stretching in addition to those for the C=C and C=O as reported by Lin *et al. (27)* and Girolami *et al.* (33) If the hfac ligand fragments and generates CF₃CO species then peaks at 1590 and 1240 cm⁻¹ corresponding to C=O and C-F stretches would appear in the IR spectrum (27).

F atom transfer from a CF_3 group on Si surface is a thermodynamically favourable process, as proposed by Capps *et al. (16, 18)*. Dissociative adsorption (14) creates CF_3 species, which generate F, probably via the following reaction pathway:

$$Cu(II)(hfac)_2(ads) \rightarrow Cu(I)(hfac)(ads) + (hfac)☼(ads)$$
$$(hfac)☼(ads) \rightarrow COCF_3 \text{ which fragments} \rightarrow CF_3(ads)$$
$$CF_3 (ads) + * \rightarrow CF_2 (ads) + F (ads)$$
$$CF_2 (ads) \rightarrow CF_2 (g)$$

where * represents an adsorption site on the Si (111)-7x7 surface and ☼ refers to the ligand that can be fragmented.

Another explanation could be the fact that under X-ray exposure some of the Cu(I)(hfac)adsorbed on Si might decompose with time as suggested by Cohen *et al.* (13).
The fact that Si $2p_{3/2}$ XPS spectrum did not detect any oxidized Si is not surprising given:
- the high probability that only mono-fluorosilicon species would appear on the surface;
- the relatively poor energy resolution of the XPS measurement;
- the low surface specificity of the XPS measurements due to the large mean free path (~ 20 Å) of the Si photoelectrons.
The above observation is consistent with that reported by Cheng *et al. (7)*.

This behaviour might explain the fact that F sticks more than O on the Si (111)-7x7surface. A similar increase in the F content with the reactant concentration was previously reported in literature (17).

4. Conclusion

Cu(hfac)$_2$ adsorption on Si(111)-7x7 at RT follows a ligand dissociative pathway with ligand fragmentation. We propose the following mechanistic approach for Cu deposition via CVD on Si(111)-7x7:the Cu(hfac)$_2$ precursor adsorbs at active sites on the Si(111)-7x7 surface as Cu(I) with some loss of ligand after ligand fragmentation. One of the two hfac ligands remains attached to Cu in a bidentate fashion while the second ligand could be fragmented.

The reduction Cu(II) $\rightarrow$ Cu(I)) takes place at electron states on adatoms (active sites) in Takayanagi's model of the Si(111)-7x7 reconstructed and atomically clean surface. This is likely because the 7x7 reconstruction creates states inside the Si band gap. This rearrangement might be held responsible for its metallic character which in turn allows the adsorption via reduction of the Cu(II) complex (Fig. 20). The fact that the precursor adsorbs as a Cu(I) complex is supported by the XPS data and by the difficulty in obtaining good images with STM for exposures of 0.04-0.1 L as reported by Horton *et al.* and our group (6, 11). The Cu atom that is released migrates until finding another Cu atom which is a favourable place for bonding. The deposited Cu acts as a nucleation site. The newly incoming Cu atoms nucleate until the cluster growth terminates when the multi-atom Cu cluster becomes covered with ligands or fragments of ligands. In order to solve this issue we plan further studies by multiple internal reflection IR spectroscopy.

The reaction products at the end of deposition at the surface are: ligands (L), fragmented ligands (L_f), Cu(I)(hfac) (Cu-L), and copper (Cu).

The proposed mechanism of cluster growth and cluster termination as retrieved from UPS/XPS data can be an answer to the so called "magic" number Cu cluster described by Horton *et al. (6)*.

References

[1] M. J. Hampden-Smith, T. T. Kodas, Polyhedron **14**(6), 699 (1995).
[2] R.L. Van Hemert, L.B. Spendlove, R. E. Sievers, J. Electochem. Soc.**112,** 1123 (1965).
[3] D. Temple, A Reisman, J. Electochem. Soc **136**, 3525 (1989).
[4] A. Jain, K. M., Chi, M. J. Hampden-Smith, T. T., Kodas, J. D., Farr, M. F. Paffett, J. Mater. Res. **7**, 261 (1992).
[5] J. Randall Creighton, J. E. Parmeter, Crit. Rev. Solid State Mater. Sci.**18**, 175 (1993).
[6] J. H. Horton, J. G. Shapter, T. Cheng, W. N. Lennard, P. R. Norton, Surf. Sci. **375**, 171 (1997).
[7] T. Q. Cheng, K. Griffiths, P. R., Norton, Puddephatt, R.J. Appl. Surf. Sci. **126**, 1303 (1998).
[8] P. Martenson, W.-X. Ni, G. V. Hansson, Phys. Rev. B **36**, 5974 (1987).
[9] Tadayyon Unpublished work.
[10] F. Ringeisen, J. Derrien, E. Daugy, Layet, J. M., P. Mathiez, F. Salvan, J. Vac. Sci. Technol. B **1**(3), 549 (1983).
[11] A. Semenov, C. Ionescu, A. Lachenwitzer, P. R. Norton, Manuscript in preparation.
[12] S. Serghini-Monim, L. L. Coatsworth, P. R. Norton, R. J. Puddephatt, Rev. Sci. Instrum. **67** (10), (1996).
[13] S. L. Cohen, M., Liehr, S Kasi, Appl. Phys. Lett. **60**(13) 30, 1585 (1992).
[14] V. M. Donnely, M. E. Gross, J. Vac. Sci. Technol. **A11**(1) 66, 73, 77 (1993).
[15] J. E. Parmeter, J Phys. Chem. **97**, 11530 (1993).
[16] N. E. Capps, N. M. Mackie, Fisher, E. R. J. Appl. Phys. **84**(9), 4741 (1998).

[17] S. -J. Ding, L. Chen, X.-G. Wan, P.-F. Wang, J.-Y. Zhang, D. W. Zhang, J. T. Wang, Materials Chemistry and Physics **71**, 125 (2001).

[18] D. M. Dobkin, M. K. Zuraw, Principles of Chemical Vapor Deposition, Kluver Academic Publishers 2003, table 5.4, p. 118 and references therein.

[19] A. Streitweiser, Jr., Streitwieser, C. H. Heathcock, Introduction to Organic Chemistry, 2nd Edition, MacMillan 1981, p. 1195.

[20] Ch. D. Wagner, A. V. Naumkin, A. Kraut-Vass, J. W. Allison, C. J. Powell, J. R. Rumble Jr., NIST Standard Reference Database 20, Version 3.4 (Web Version).

[21] J. F. Moulder, W. F. Stickle, P. E. Sobol, K. D. Bomben, Handbook of X-ray Photoelectron Spectroscopy, Perkin-Elmer Corp., Eden Prairie (1992).

[22] M. P Seah, Surf. Intreface Anal. **31**, 72139 (2001) – E. T. Mickelson, I. W. Chiang, J. L. Zimmerman, P. J. Boul, J. Lozano, J. Liu, R. E. Smalley, R. H. Hauge, J. L. Margrave, J. Phys. Chem. B **103**, 4319 (1999).

[23] D. C. Frost, A. Ishitani, C. A. McDowell, Mol. Phys. **24**(4), 861 (1972).

[24] N. Sulitanu, Physics of the Solid State, University Press"Alexandru Ioan Cuza" 183 (1997).

[25] R. J. Hammers, M. R., Tromp, J. E. Demuth, Phys. Rev. Lett. **56**(18), 1972 (1986).

[26] S. L. Cohen, M. Liehr, S. Kasi, Appl. Phys. Lett. **60**(1), 50 (1992).

[27] W. Lin, C. Wiegand, R. Nuzzo, G-S. J. Girolami, Am. Chem. Soc. **118**(25), 5977 (1996).

[28] M., Ikeda, S., Iwamoto, N. Nagashima, Electronics and Communications in Japan, Part 2, **83**(7), 43 (2000).

[29] A. Ermolieff, F. Martin, A. Amouroux, S. Marthon, J. F. M. Westendorp, Semicond. Sci. Techno **l.6**, 98 (1991).

[30] F. Rocaforte, F. La Via, V. Rainieri, European Solid-State Device Research Conference (2002) 545.

[31] E. Z. Kurmaev, et al., Bartkowski, S. et al., Greaves, C. et al., Novikov, D. L. Phys. Rev. B **52**(4), 2392 (1995).

[32] E. Z. Kurmaev, A. Moewes, D. L. Ederer, H. Ishii, K. Seki, M. Yanagihara, F. Okino, Touhara, H. The Advanced Light Source - Home page. Berkeley Lab · 1 Cyclotron Rd · MS6R2100 · Berkeley, CA 94720, USA

[33] G. S. Girolami, P. M. Jeffries, L. H. Dubois, J. Am. Chem. Soc.**115,** 1015 (1993).

[34] C. Ionescu, M. Ionescu, I. Ciuca, Optoelectron. Adv. Mater. – Rapid Commun. **5**(7), 722 (2011).

[35] C. Ionescu, M. Ionescu, I. Ciuca, Optoelectron. Adv. Mater. – Rapid Commun. **5**(8), 883 (2011).

_____
[*]Corresponding author: cionescuphd@gmail.com